Blast waves produced by interactions of femtosecond laser pulses with water

Y. T. Li, J. Zhang,* H. Teng, K. Li, X. Y. Peng, Z. Jin, X. Lu, Z. Y. Zheng, and Q. Z. Yu
Laboratory of Optical Physics, Institute of Physics, Chinese Academy of Sciences, Beijing 100080, People's Republic of China
(Received 19 March 2002; revised manuscript received 21 January 2003; published 12 May 2003)

The behaviors of the blast waves produced by femtosecond laser-water interactions, and the blast waves induced by laser self-focusing in air, have been investigated using optical shadowgraphy at a maximum intensity of 1×10^{16} W/cm^2. The temporal evolution of the blast wave launched by the water plasma can be described by a planar blast wave model including source mass. An aneurismlike structure, due to the quick propagation inside a hollow channel formed by laser self-focusing, is observed. The expansion of the channel in air is found to agree with a cylindrical self-similar blast wave solution.

DOI: 10.1103/PhysRevE.67.056403 PACS number(s): 52.35.Tc, 52.38.Hb

I. INTRODUCTION

When a high-intensity laser beam is focused on matter, the transient and localized energy deposition leads to a high-temperature plasma and a successive blast wave moving outward into the surrounding medium. A self-similar blast wave model proposed by Sedov [1] and Zel'dovich [2], which is valid for an intensively instant point explosion and zero initial source mass, is widely used to interpret the behaviors of the blast wave generated by laser-solid [3–6] and laser-cluster interactions [7,8]. Freiwald modified the model to include the explosive mass [9,10]. Long laser pulses were applied widely in previous studies on laser-produced blast wave. The recent developments of laser technology to produce ultrashort pulse make it possible to compare the femtosecond laser-induced blast wave with the Sedov theory.

In addition, some groups have investigated the behaviors of the blast waves generated by laser-induced breakdown inside liquid [11–14]. However, there is very little knowledge about the behaviors of blast waves generated on a liquid-air interface irradiated by laser pulses. In this paper, we investigate the evolution of the blast waves produced by femtosecond laser-water interaction on the water surface, and the evolution of a low-density channel in air due to laser self-focusing using optical shadowgraphy at a high laser intensity. The results show that the waves follow higher power laws than a self-similar spherical blast wave model. An aneurismlike structure on the top of the blast wave is also observed and its generation mechanism is analyzed.

II. EXPERIMENT

The experimental setup is illustrated schematically in Fig. 1. A chirped pulse amplification Ti:sapphire laser that delivers up to 5 mJ, 150 fs pulses at a wavelength of 800 nm was used. The linearly polarized laser pulses were focused with an $f=40$ mm lens onto a distilled water surface in air, yielding a maximum peak intensity of about 1×10^{16} W/cm^2.

A small portion of the laser beam split from the main beam, after being frequency doubled to 400 nm, was used as a probe. The expansion of the plasma and the resultant blast wave was imaged on a 16 bit, 512×512 pixels CCD camera with a $14\times$ magnification. An assembly of neutral filters and interference filters with a narrow bandwidth singled out the 400-nm probe beam from the background emission. In some shots, a 100-μm-diameter thread was placed at the back focus of the imaging lens to improve the contrast by blocking most of the undeflected probe light. Varying the delay of the probe beam with respect to the interaction beam on successive shots permitted mapping of the evolution of the blast waves. The time resolution was determined by the duration of the probe beam of about 150 fs.

The transmission energy was measured using a calorimeter in the laser propagation direction with a collective angle of 60°. Other diagnostics included hot electron measurements with an array of LiF thermoluminescence dosimeters

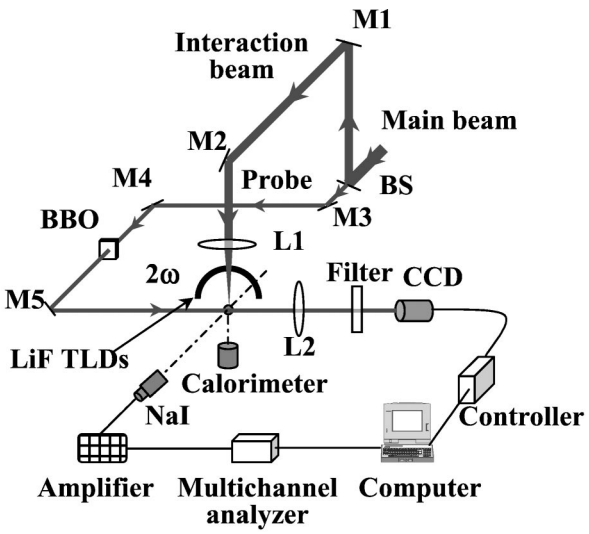

FIG. 1. The experimental layout. A small portion of the laser beam split from the main beam was frequency doubled and used to probe the blast wave. $M1$-$M5$ are reflective mirrors and BS represents the beam splitter. $L1$ and $L2$ are two lenses, which were used to focus the interaction beam on the water surface and image the plasma on CCD, respectively. The angular distribution of hot electrons emitted from the plasma was detected by an array of LiF detectors surrounding the plasma. The NaI system was used to measure the spectra of hard x rays.

*Author to whom correspondence should be addressed. Electronic address: jzhang@aphy.iphy.ac.cn

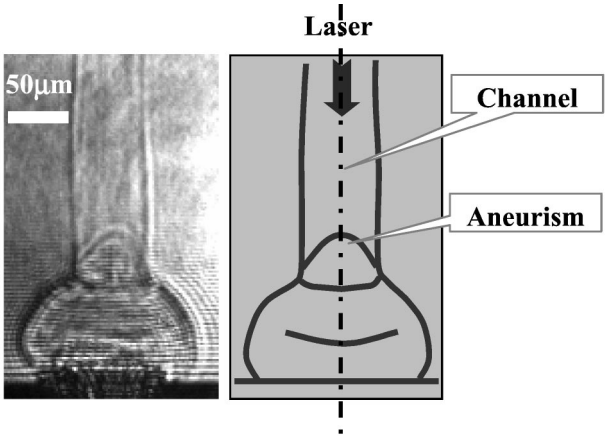

FIG. 2. A typical shadowgram of the blast wave taken at a delay time of 10 ns. The right one is an artificial sketch to guide the sightline.

[15], and hard x-ray measurements with a γ-ray spectrometer, which consisted of an NaI detector, a photomultiplier, an amplifier, and a multichannel energy analyzer [16]. Intense hard x-ray photon and electron emissions were also observed in the water plasma when multiple pulses with long separation time were used. These results will be presented elsewhere [17].

III. RESULTS AND DISCUSSION

A. Characteristics of the blast waves produced by femtosecond laser-water plasmas

Figure 2 shows a typical shadowgram of the blast wave taken at a delay time of 10 ns. An artificial sketch is also drawn on the right to lead the sightline. The femtosecond laser pulse with an energy of 3 mJ enters the image from the top. Note the main features in Fig. 2: generation of a hemispherical blast wave launched from the focal spot, an aneurismlike structure on the top of the wave, and a cylindrical blast wave trajectory generated before the laser pulse strikes on the water surface.

At first, we will discuss the evolution of the blast waves emitted from the water plasma. Figure 3 shows the images of the blast waves above the water surface at (a) 3 ns, (b) 4.7 ns, (c) 11.3 ns, (d) 16.9 ns, and (e) 30 ns produced by a laser beam with an energy of 3 mJ. The laser beam is incident from the top. The fringes near water surface are due to the diffractions of water surface. A half-circle dashed line whose center locates at the focal spot is overlaid on the shadowgram

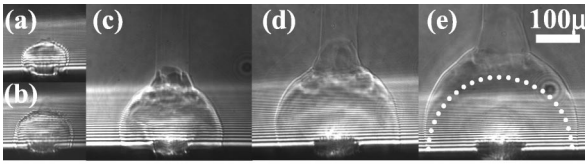

FIG. 3. Images of the blast waves above the water surface at 3 ns (a), 4.7 ns (b), 11.3 ns (c), 16.9 ns (d), and 30 ns (e). The laser beam is incident from the top.

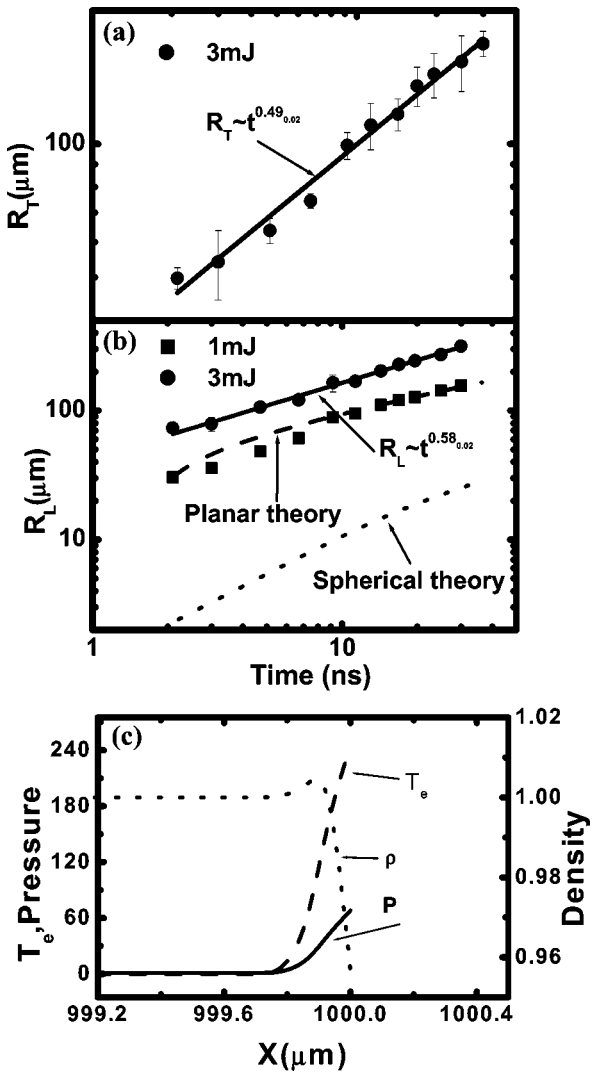

FIG. 4. Evolution of the blast waves produced by the femtosecond laser ablation of water as a function of time: transverse expansion for a 3-mJ laser energy (a), and longitudinal expansion for two laser energies, 3 mJ (circle) and 1 mJ (square) (b). The dashed line and the dotted line are theory curves for planar blast wave and spherical blast wave considering the initial source mass, respectively. (c) The hydrodynamical simulation results of the spatial profiles of the mass density ρ, pressure p, and electron temperature T_e are shown at the end of the laser pulse.

in Fig. 3(e). It is obvious that the blast wave propagates faster than an ideal spherical wave. The transverse expansion of the blast wave front for a 3-mJ laser energy, and the longitudinal expansion for 3-mJ (circle) and 1-mJ (square) laser energies are plotted as a function of time in Figs. 4(a) and 4(b), respectively. In the figures, R_T is denoted as the transverse expansion radius of the blast wave front parallel to the water surface, and R_L is the longitudinal expansion radius in the normal direction of water surface. The data from five measurements were averaged. The error bars correspond to the shot-shot fluctuations. For the transverse evolution, an allometric fit of the experimental data shows a dependence of $R_T \sim t^{0.49 \pm 0.02}$. For the longitudinal evolution, the data are

fitted by $R_L \sim t^{0.58\pm0.02}$ for 3 mJ and $R_L \sim t^{0.59\pm0.03}$ for 1 mJ (not shown).

It is well known that the evolution of the radius of a blast wave with time proposed by Sedov can be written as [1]

$$R^{n+2} = \alpha(\gamma)\frac{E_0}{\rho_1}t^2, \tag{1}$$

where E_0 is the original energy deposited per unit length in the cylinder, ρ_1 is the undisturbed mass density, α is a coefficient dependent on the adiabatic constant of the gas, γ, n is 1, 2, and 3 for plane, cylindrical, and spherical wave propagations. Sedov's theory indicates that the blast wave produced in our experiments is in agreement with a cylindrical blast wave for the transverse expansion, and is very close to a planar blast wave for the longitudinal expansion. Both the expansion directions deviate from a spherical blast wave predicted from Eq. (1). Similar results were also observed earlier [18,19].

Sedov's theory is valid only when the initial explosive mass is much less than the mass of the background gas swept over by the blast wave. We estimate the explosive mass of water to be 2.82×10^{-10} g by the hydrodynamic simulation of the femtosecond laser-water interaction (see next). This mass is equivalent to an air mass encompassed by a half-spherical blast wave with a radius of ~ 50 μm. Therefore, Sedov's theory cannot well describe our results of the blast wave, whose radius is less than 300 μm within the time observed.

Freiwald proposed an approximate theory including source mass for both spherical blast [9] and planar blast [10]. The spherical blast expansion in the near-target regime where the source mass is not negligible can be expressed analytically as

$$t = E_0^{-1/2}C_1^{1/2}\left(\frac{C_1}{C_2}\right)^{1/2}\left[\frac{3}{5}\frac{1}{3^{1/4}}F(\phi,75°) + \frac{2}{5}\beta(1+\beta^3)^{1/2} - 0.842\right], \tag{2}$$

where

$$C_1 = \frac{2m_s}{(\gamma+1)^2},$$

$$C_2 = \frac{8\pi}{3}\rho_1\left(\frac{2}{(\gamma+1)^2} + \frac{1}{\gamma^2-1}\right),$$

$$\beta = R\left(\frac{C_2}{C_1}\right)^{1/3},$$

$$\phi = \cos^{-1}\left(\frac{\sqrt{3}-1-\beta}{\sqrt{3}+1+\beta}\right),$$

m_s is the initial mass, F is the incomplete elliptic integral of the first kind. The expansion of the planar blast wave with source mass is governed by

$$\frac{dR}{dt} = \left(\frac{E_0}{C_4 + C_5R^3}\right), \tag{3}$$

where

$$C_4 = \frac{m_s}{2}\left(\frac{1}{\gamma+1}\right)^2,$$

$$C_5 = 2\pi\rho_1\left(\frac{1}{\gamma^2-1} + \frac{4}{(\gamma+1)^2}\right).$$

We modify C_5 by rewriting the expression of the background gas mass to suit our experimental blast wave. The theoretical expansion of the planar blast is obtained by solving Eq. (3) with initial value problem. The comparison of Freiwald's theory with experimental results for 1-mJ laser pulse is also shown in Fig. 4(b). There exists a considerable amount of discrepancy between Freiwald's spherical blast model (dotted line) and experimental data even that the source mass is included. However, we find that Freiwald's planar blast wave theory agrees well with the experimental points when E_0 is set to be 0.15 mJ (see the dashed line). This indicates that the blast wave observed propagates closer to a plane blast wave instead of a spherical one, and that $\sim$15% of the incident laser energy converts into the blast energy. It can be expected that the blast wave will decay to a spherical wave with the increasing propagation distance as the ambient gas accretion and the energy dissipation.

The higher power laws observed in our experiments may be due to the high intensity used and the nature of the femtosecond laser-matter interactions. To understand the initial explosive conditions of the blast wave, we use a one-dimensional two-temperature hydrodynamics code (MED103) [20] to simulate the behavior of the water plasma generated by 150-fs laser pulses at an intensity of 5×10^{15} W/cm^2. Figure 4(c) shows snapshots of the spatial profiles of the mass density ρ, pressure p, and electron temperature T_e at the end of the laser pulse. The water surface was located at 1000 μm; the laser pulse was incident from the right. When the laser pulse ends, a 68-Mbar peak pressure is produced. The maximum electron temperature is 244 eV. This high-temperature and high-pressure plasma will push the surrounding gas to generate intense shock wave in the air. We also simulate the case for nanosecond laser pulse that was used to produce blast wave in previous experiments widely. We find that the pressure and the temperature of the femtosecond laser-produced plasma are much higher than that of the nanosecond laser case at the same energy (the electron temperature is $\sim$100 ev and the pressure is $\sim$1 Mb for 1-ns laser). That is to say the femtosecond laser plasma will lead to a more intense explosion and will result in a

higher velocity blast wave expansion than that formed by long laser pulse at the same energy. The high-pressure and the high Mach number measured (~ 20) will make the blast wave to be strongly forward peaked. On the other hand, for an ultrashort laser-produced plasma, the plasma expansion during the pulse can be expressed as $c_s\tau$, where c_s is the ion velocity ($\sim 10^7$ cm/s) and τ is the pulse width. One can see that the scale of plasma during the interaction is several tens of nanometers, which is much less than the laser focal spot. This intrinsically planar interaction geometry may also be related with the behavior of the planar blast wave at early times.

Other reasons for the high power law is partial ionization and dynamic source effect [21]. The partial ionization induced by the blast wave front can accelerate the propagation in all directions. The nonadiabatic dynamic effect may increase the expansion velocity especially in the normal direction of the target surface. This may result in the higher velocity in the longitudinal direction than that in the transverse direction.

Second, we discuss the formation of the aneurism structure. The hollow channel in air plays a key role in the formation of the aneurism. From the blast wave theory, we know that the velocity of a blast wave dR/dt increases with the decrease of the ambient density. Therefore, the blast wave originating from the water plasma inside the low-density channel propagates more quickly than the outside part. This leads to the aneurism structure observed in our experiments. Stamper *et al.* also observed an aneurism production using 4 ns, ~ 100 J Nd-glass laser beams to irradiate foil targets at $\sim 10^{13}$ W/cm^2 in a low-pressure ambient gas, where a channel was formed by laser heating of the ambient gas through the inverse bremsstrahlung [22]. In our experiments, we believe that the initial ionization processes are different from theirs for our high-intensity and short-duration laser pulse because the laser field is comparable to the column potential.

B. Cylindrical blast waves produced by laser self-focusing in air

Now, we examine more closely the behavior of the blast wave produced by femtosecond laser pulses in air. When a femtosecond laser pulse is focused in air, a hot, elongated filament is formed due to the Kerr effect because the laser power is much higher than the self-focusing threshold (the critical power for self-focusing is $P_{cr}=\lambda^2/2\pi n_2=2$ GW, where λ is laser wavelength and n_2 is nonlinear refractive index. At atmospheric pressure, for air $n_2=3.2\times 10^{-19}$ cm^2/W), a blast wave is induced as a result of the high pressure exerted by the high-temperature filamentlike plasma. Figure 5 shows the shadowgrams of the blast waves produced by laser breakdown at 3 ns, 11.3 ns, 16.9 ns, and 24.9 ns. The geometry of the laser beam waist ($1/e^2$ contours) in the same scale as the shadowgrams is also shown for comparison. Laser is incident from the top. The abrupt jumps of the brightness in the shadowgrams indicate the shells of the waves.

Figure 6 shows the radial evolution of the blast wave

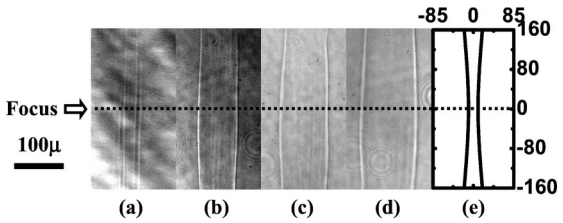

FIG. 5. Shadowgrams showing the evolution of the blast waves in air produced by a 3-mJ laser energy as a function of time: 3 ns (a), 11.3 ns (b), 16.9 ns (c), and 24.9 ns (d). The geometry of the laser beam waist ($1/e^2$ contours) in the same scale as the shadowgrams is also shown for comparison (e).

trajectory at the focal spot as a function of time for a 3-mJ laser energy. The data from five measurements were averaged. The error bars correspond to the shot-shot fluctuations. The experimental data are best fitted by an allometric function $R(t)\sim t^{0.49\pm 0.01}$. This indicates that the blast wave expansion in air follows a cylindrical blast wave solution. From Eq. (1), the conversion efficiency of total laser energy to the blast wave is estimated to be less than 1%. This value is lower than the total absorption by air plasma, which is measured to be 6% by an energy calorimeter. This indicates that most of the energy absorbed by plasmas is transformed to other energy forms such as ionization energy, instead of the kinetic energy of blast wave. Compared with the previous laser-ablation experiments using long pulses, the conversion efficiency of laser pulse into blast waves is much lower for femtosecond laser-air interactions. In the nanosecond scale laser-air interactions, the plasma still absorbs energy from the succeeding part of the laser pulse through inverse bremsstrahlung after the air is ionized by the leading part of the pulse. Therefore, more laser energy can be deposited and transferred to the blast wave energy. However, for the case of femtosecond pulse, less energy can be absorbed from the tail of the femtosecond pulse.

IV. CONCLUSION

In summary, blast waves produced by femtosecond laser-water interaction have been investigated using an optical shadowgraphy technique. The temporal evolution of the blast

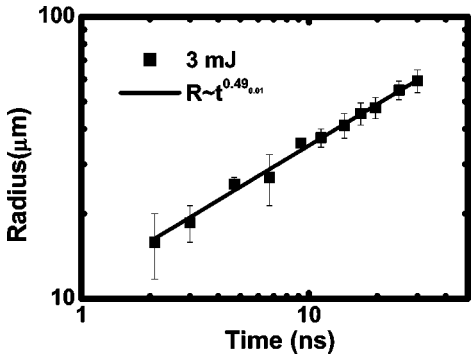

FIG. 6. Radial evolution of the blast waves in air as a function of time for a 3-mJ laser energy. The line is an allometric fit of the experimental data.

wave formed by the water plasma follows a planar blast wave model including the source mass. An aneurismlike structure, due to the quick propagation inside the air channel that is formed by laser filamentation, is observed. The blast wave in air is found to agree with a cylindrical self-similar blast wave solution.

ACKNOWLEDGMENTS

This work was supported by the NSFC (Project Nos. 10204023, 10075075, and 10176034), the K. C. Wang Education Foundation (Hong Kong), the National High-Tech ICF program, and the NKBRSF (Grant No. G1999075206).

[1] L.I. Sedov, *Similarity and Dimensional Methods in Mechanics* (Infosearch LTD, London, 1959).
[2] Ya.B. Zel'dovich and Yu.P. Raizer, *Physics of Shock Waves and High-Temperature Hydrodynamic Phenomena* (Academic, New York, 1966).
[3] S.J. Lee, K. Imen, and S.D. Allen, J. Appl. Phys. **74**, 7044 (1993).
[4] G. Callies, P. Berger, and H. Hugel, J. Phys. D **28**, 794 (1995).
[5] T. Zyung, H. Kim, J.C. Postlewaite, and D.D. Dlott, J. Appl. Phys. **65**, 4548 (1989).
[6] K.S. Budil, D.M. Gold, K.G. Estabrook, B.A. Remington, J. Kane, P.M. Bell, D. Pennington, C. Brown, S. Hatchett, J.A. Koch, M.H. Key, and M.D. Perry, Rev. Sci. Instrum. **70**, 806 (1999).
[7] J. Zweiback and T. Ditmire, Phys. Plasmas **8**, 4545 (2001).
[8] M.J. Edwards, A.J. MacKinnon, J. Zweiback, K. Shigemori, D. Ryutov, A.M. Rubenchik, K.A. Keilty, E. Liang, B.A. Remington, and T. Ditmire, Phys. Rev. Lett. **87**, 085004 (2001).
[9] D.A. Freiwald and R.A. Axford, J. Appl. Phys. **46**, 1171 (1975).
[10] D.A. Freiwald, J. Appl. Phys. **43**, 2224 (1972).
[11] C.E. Bell, and J.A. Landt, Appl. Phys. Lett. **10**, 46 (1967).
[12] F. Docchio, P. Regondi, M.R.C. Capon, and J. Mellerio, Appl. Opt. **27**, 3661 (1988).
[13] A.G. Doukas, A.D. Zweig, J.K. Frisoli, R. Birngruber, and T.F. Deutsch, Appl. Phys. B: Photophys. Laser Chem. **53**, 237 (1991).
[14] A. Vogel, S. Busch, and U. Parlitz, J. Acoust. Soc. Am. **100**, 148 (1996).
[15] L.M. Chen, J. Zhang, H. Teng, Q.L. Dong, Z.L. Chen, T.J. Liang, L.Z. Zhao, and Z.Y. Wei, Phys. Rev. E **63**, 046403 (2001).
[16] P. Zhang, J.T. He, D.B. Chen, Z.H. Li, Y. Zhang, J.G. Bian, L. Wang, Z.L. Li, B.H. Feng, X.L. Zhang, D.X. Zhang, X.W. Tang, and J. Zhang, Phys. Rev. E **57**, R3746 (1998).
[17] Y. T. Li, J. Zhang, H. Teng, T. J. Liang, X. Y. Peng, X. Lu, Y. J. Li, and X. W. Tang, Phys. Rev. Lett. **90**, 165002 (2003).
[18] A. Gupta, B. Braren, K.G. Casey, B.W. Hussey, and R. Kelly, Appl. Phys. Lett. **59**, 1302 (1991).
[19] S.H. Jeong, R. Grief, and R.E. Russo, Appl. Surf. Sci. **127**, 1029 (1998).
[20] J.P. Christiansen, D.E.T.F. Ashby, and K.V. Roberts, Comput. Phys. Commun. **7**, 271 (1974).
[21] K.R. Chen, J.N. Leboeuf, R.F. Wood, D.B. Geohegan, J.M. Donato, C.L. Liu, and A.A. Puretzky, Phys. Rev. Lett. **75**, 4706 (1995).
[22] J.A. Stamper and B.H. Ripin, Phys. Fluids **31**, 3353 (1988).